Supporting Information

Room-temperature selective NO_2 sensing using porous TiO_2 nanorods via a humidity-mediated conduction

Young Geun Song[1], Suk Yeop Chun[2,3], Yumin Park[2,3], Ilho Myeong[4], Young-Seok Shim[5,], and Chong-Yun Kang[2,3,*]*

[1] Department of Electronic Engineering, Tech University of Korea, Siheung, 15073, Republic of Korea

[2] KU-KIST Graduate School of Converging Science and Technology, Korea University, Seoul, 02841, Republic of Korea

[3] Electronic and Hybrid Materials Research Center, Korea Institute of Science and Technology (KIST), Seoul 02791, Republic of Korea

[4] Department of Electronics Engineering, Myongji University, Yongin, 17058, South Korea

[5] School of Energy, Materials and Chemical Engineering, Korea University of Technology and Education (KOREATECH), Cheonan 31253, Republic of Korea

E-mail: ysshim@koreatech.ac.kr, cykang@kist.re.kr

Keywords: metal-oxide, gas sensor, room-temperature, humidity-mediated, TiO_2, NO_2

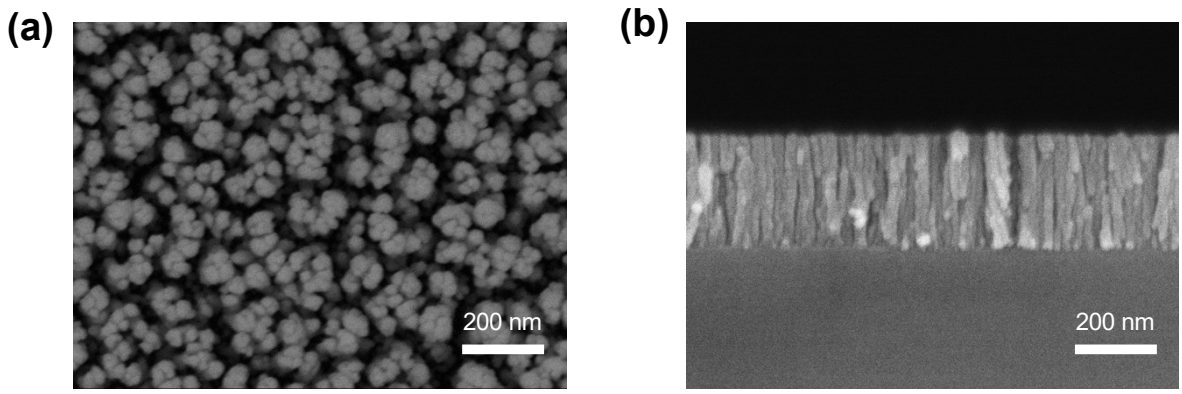

Fig. S1 Higher magnification (a) Plane and (b) cross-sectional SEM image of TiO_2 NRs.

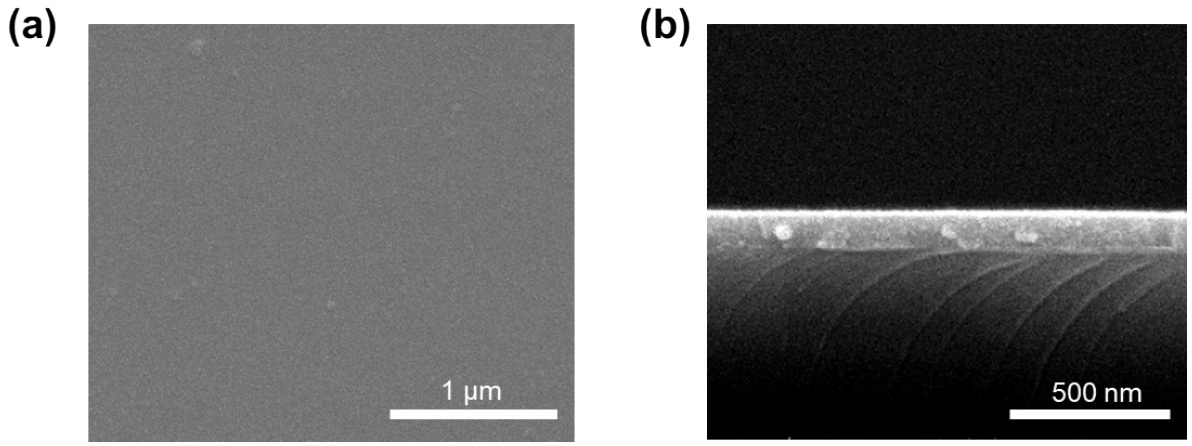

Fig. S2 (a) Plane and (b) cross-sectional SEM images of TiO_2 thin films. XRD patterns of the TiO_2 thin films.

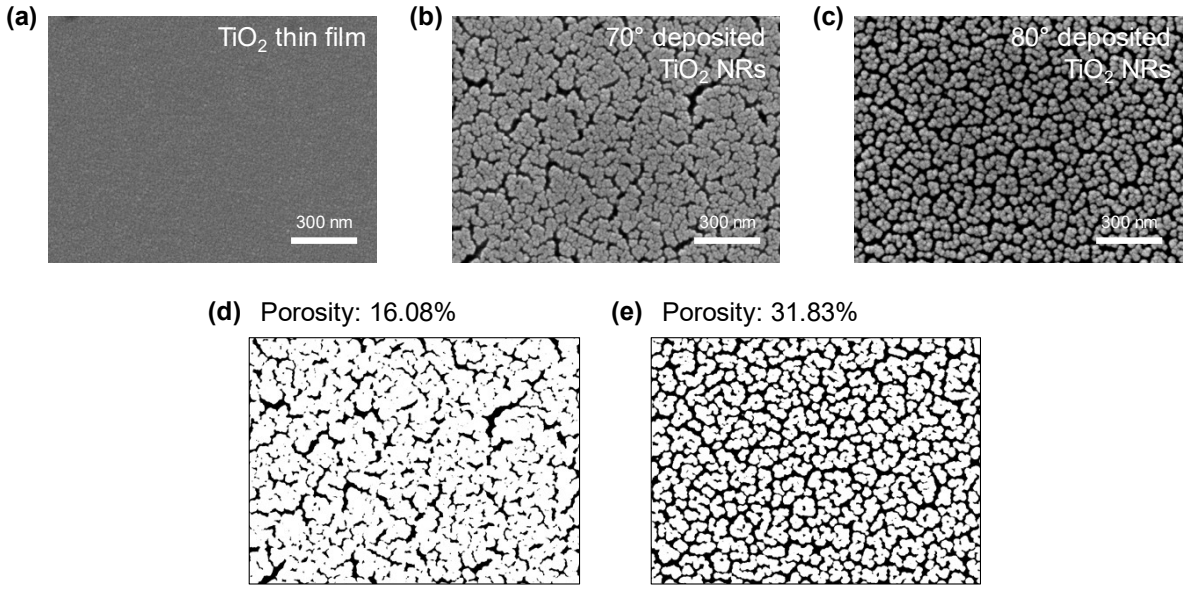

Fig. S3 Top-view SEM images of (a) TiO_2 thin film, (b) NRs deposited at 70°, and (c) NRs deposited at 80°. Corresponding contrast-enhanced binary images of (d) 70° and (e) 80° samples highlighting the increased in void fraction with increasing deposition angle.

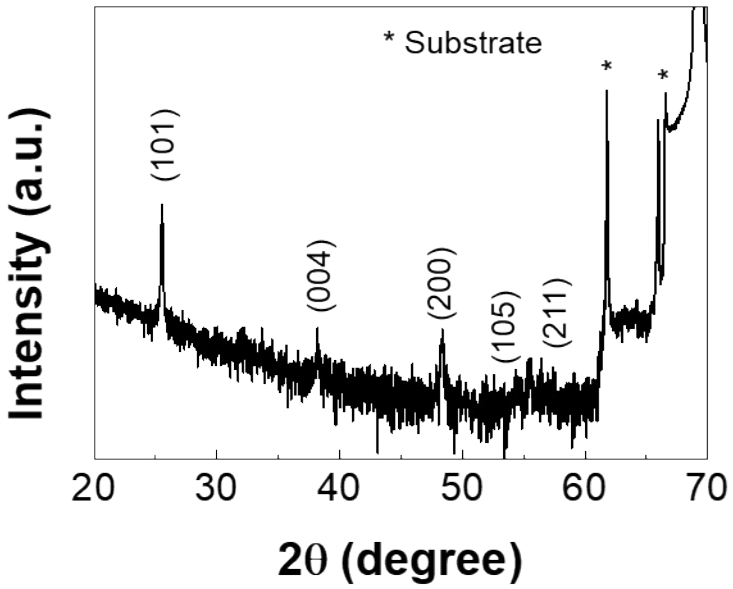

Fig. S4 XRD pattern of TiO_2 NRs, showing diffraction peaks corresponding to the anatase phase (JCPDS no. 21-1272) without detectable impurity phases.

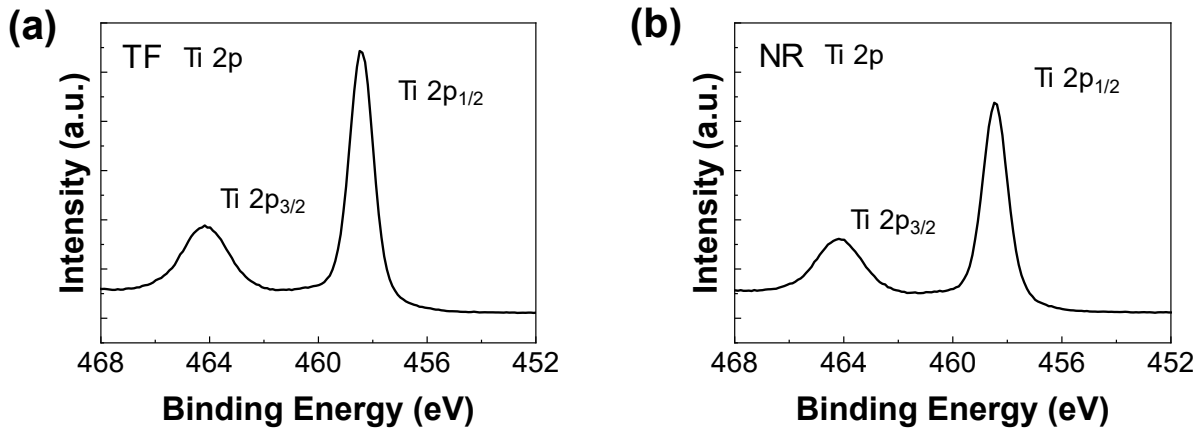

Fig. S5 XPS spectra of Ti 2p peaks for TiO_2 (a) thin film and (b) NRs.

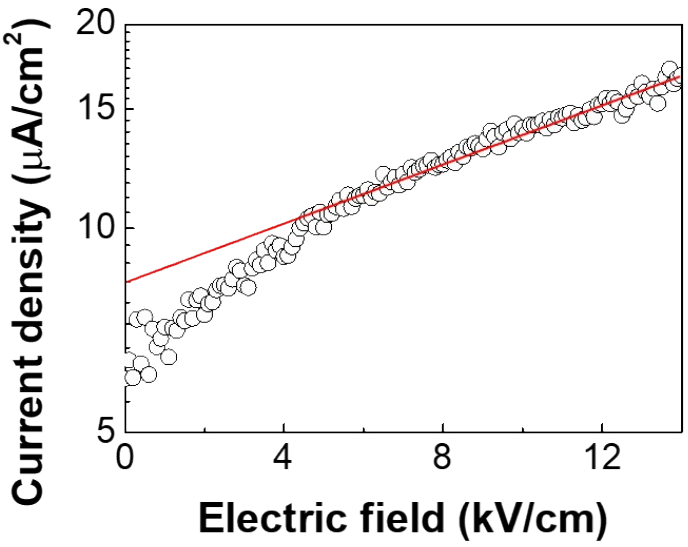

Fig. S6 Current density–electric field (J–E) characteristics of TiO_2 nanorod sensors under dry air conditions.

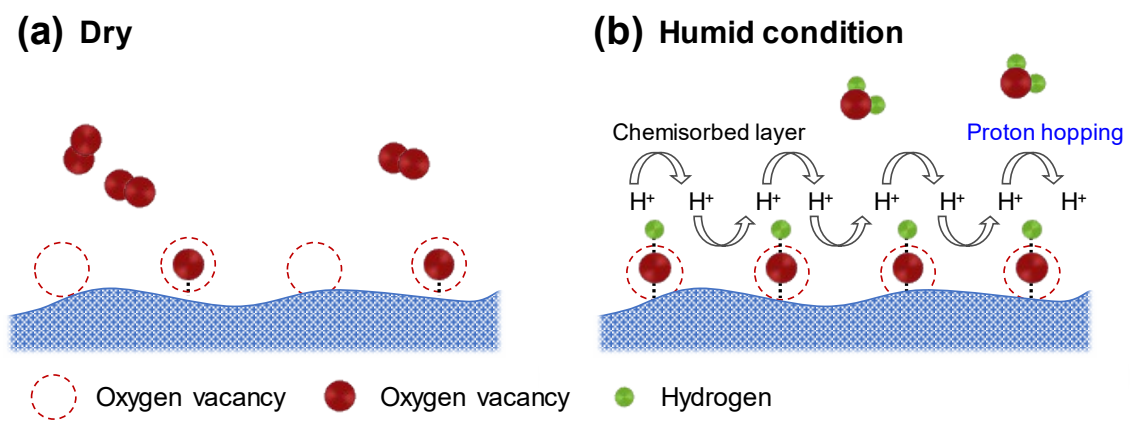

Fig. S7 Schematic illustrations of the surface states of TiO_2 under (a) dry condition and (b) humid condition, where adsorbed water dissociates into hydroxyl groups, forming a chemisorbed layer that enables proton hopping through hydrogen-bonded networks

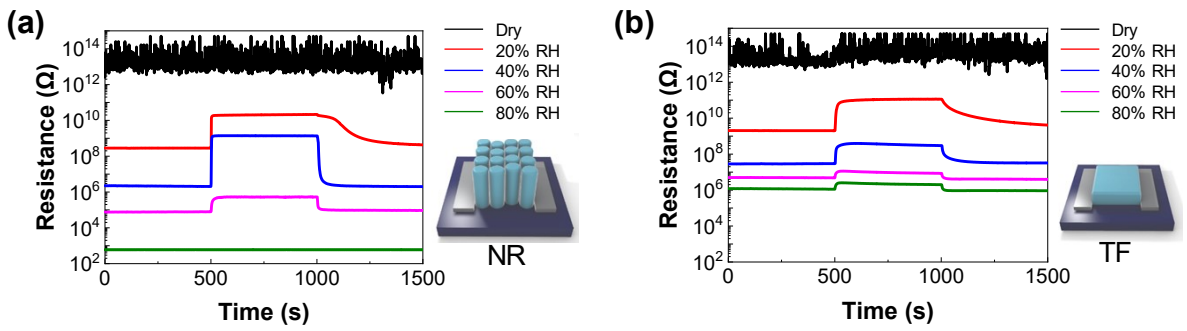

Fig. S8 Resistance transients of (a) TiO_2 NRs and (b) thin films upon exposure to 2 ppm NO_2 at room temperature under 5 V, measured as a function of relative humidity.

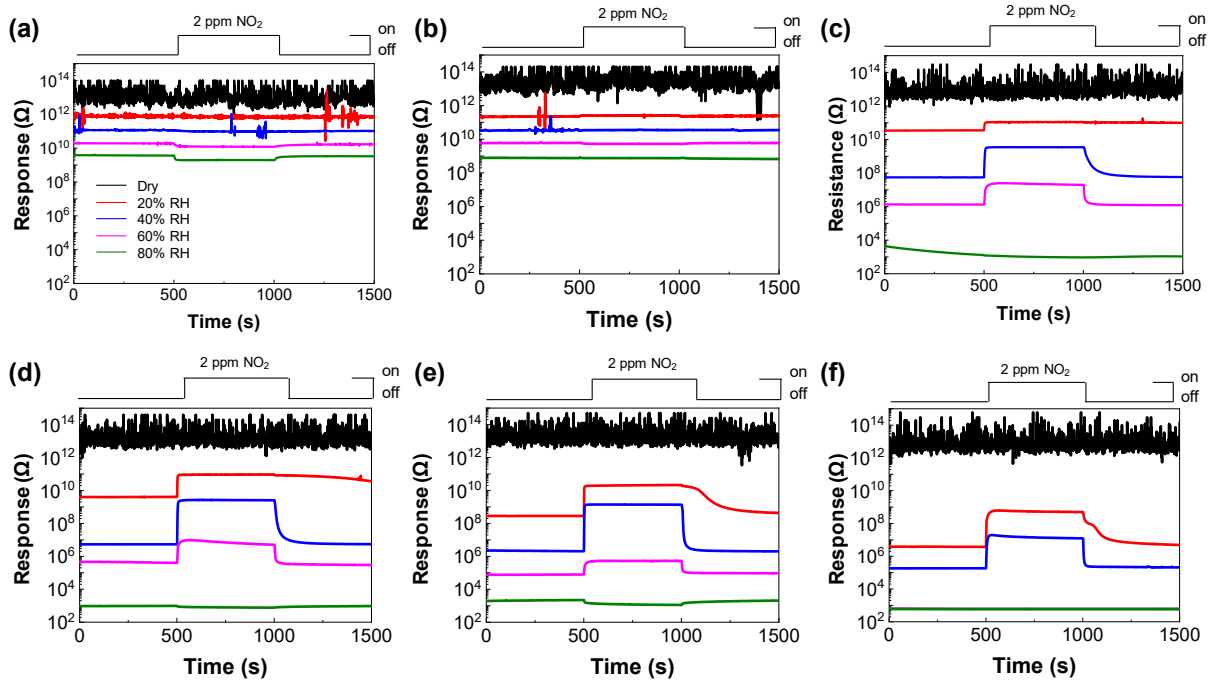

Fig. S9 Resistance transients of TiO_2 NRs exposed to 2 ppm NO_2 under different relative humidity levels (0%, 20%, 40%, 60%, and 80%) at room temperature: (a) 1 V, (b) 2 V, (c) 3 V, (d) 4 V, (e) 5 V, and (f) 6 V applied bias conditions.

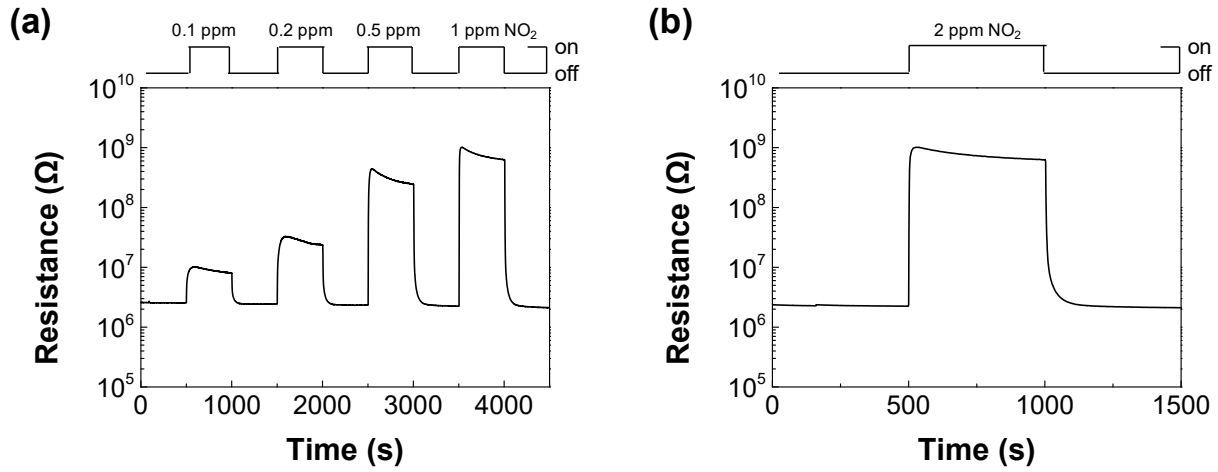

Fig. S10 Resistance transients of TiO_2 NR sensors at room temperature under 5 V bias and 40% RH. (a) Responses to varying NO_2 concentrations of 0.1, 0.2, 0.5, and 1 ppm, and (b) response to 2 ppm NO_2, demonstrating clear concentration-dependent sensing behavior.

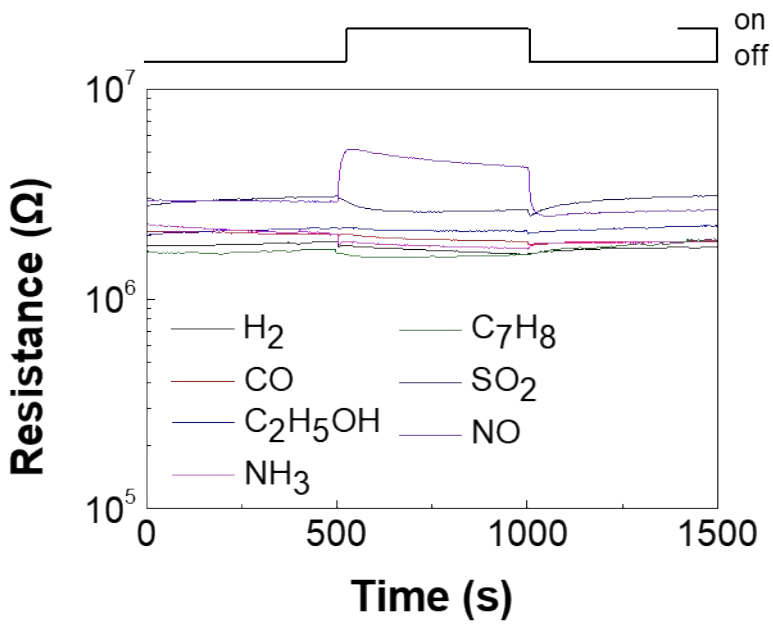

Fig. S11 Resistance transients of TiO_2 NR sensors exposed to 10 ppm of interfering gases (H_2, CO, C_2H_5OH, NH_3, C_7H_8, SO_2, and NO) at room temperature and 40% RH under an applied bias of 5 V, demonstrating negligible responses compared to NO_2.

Table S1. Sensing performance of room temperature NO_2 sensors

Sensing material	Detection limit	NO_2 Response	Recovery time	RH window	Ref.
SnO_2 nanorods	132.3 ppt	3.97 @ 200 ppb	25.7s @ 5 ppm	20% RH	[1]
Self-powered Au@SnO_2 nanorods	4.32 ppb	6.39 @ 1 ppm	6s @ 1 ppm	20% RH	[2]
TiO_2 nanorods	505 ppt	2.17 @ 100 ppb	4 s @ 2 ppm	20–40% RH	This work

References

1. Song, Y. G.; Shim, Y. S.; Suh, J. M.; Noh, M. S.; Kim, G. S.; Choi, K. S.; Jeong, B.; Kim, S.; Jang, H. W.; Ju, B. K., *Small* **2019,** *15* (40), 1902065.

2. Song, Y. G.; Jung, I.; Shin, J.; Shim, Y.-S.; Kim, G. S.; Ju, B.-K.; Kang, C.-Y., *Sensors and Actuators B: Chemical* **2021,** *332*, 129481.